

Large-scale CFD Simulation for Classification of Climatopes in Tokyo's 23 Wards

Project Representative

Yasunobu Ashie Environmental Research Group, Building Research Institute

Authors

Kohin Hirano^{*1}, Takaaki Kono^{*1} and Yasunobu Ashie^{*1}

^{*1} Environmental Research Group, Building Research Institute

In order to allow heat island countermeasures to be optimally used in urban planning, authors have developed an analysis system running on the Earth Simulator for urban thermal environment studying. This system can simulate the atmospheric environment considering radiative heating, fluid dynamics as well as artificial pavement, building shapes and anthropogenic heat. Using this system, the thermal environment in a 10 km square area of central Tokyo and a 33 km square area included the whole Tokyo's 23 wards have been analyzed with 5 m resolution in the past. In this year, we performed a principal component analysis on the result of the 33 km square area simulation to find the thermal features of different types of districts. The classification was conducted according to urban information and environmental factors such as ratio of open green space coverage, building coverage, building height, wind velocity and temperature near ground surface, etc.

Keywords: heat island, CFD, classification, cluster analysis, principle component analysis

1. Introduction

The heat-island phenomenon has become a serious social issue in cities. The national and municipal governments and various companies have prepared guidelines, introduced technologies, and taken countermeasures. However, to solve the issue, highly precise numerical simulations need to be performed to reproduce the actual phenomenon and assess the effects of measures. The authors have improved the standard k - ϵ model, aiming to develop a large-scale high-resolution system of numerical analysis for predicting the thermal environment at all scales ranging from the periphery of a building to an entire city by using the computational performance of the Earth Simulator. The authors have successfully conducted the computational fluid dynamics (CFD) simulations in an area of 10 km square covering most of the coast of Tokyo, and an area of 33 km square covering the whole 23 wards of Tokyo^{[1],[2],[3]}. To systematically organize the characteristics of the microclimate in each city district, the districts were classified by type based on the results of the CFD analysis.

This paper describes the basic equations of the numerical model and the results of classifying the districts in Tokyo's 23 wards.

2. Numerical model

The CFD model used in this study was based on a standard k - ϵ model, which is widely used in engineering for ana-

lyzing turbulent flows of fluids. The basic equations and constants of the model are shown in Fig. 1. The FAVOR method was used to recognize the complicated locations and shapes of buildings. The effects of potential temperature, Coriolis force and vapor buoyancy were newly introduced into the equations to reproduce various city-scale phenomena. The pressure term, which appears in an ordinary equation of energy transfer, was combined with that of potential temperature and expressed together in the equation of energy transfer as a potential term. Since sonication requires processing at short time intervals, the SIMPLEC method was used to solve the pressure in the equation of motion to ensure numerical stability.

2.1 Handling radiation

The actual heat environments in cities are non-steady and constantly change along with sunshine and wind velocity. Cities have complicated geometrical configurations, making it very complicated to numerically monitor radiation and heat accumulation and to analyze a large area as a whole using a non-steady model. In this study, sunny and shaded zones were not determined in detail, but the temperature of the ground surface in each zone was simply estimated from the ground cover state. Prior to the estimation, non-steady calculations for an entire day were performed using a linear heat balance model to clarify the relationship between temperature and the conditions of sunshine and ground cover. Humidity at the

【Equation of continuity】

$$G_v \frac{\partial \rho}{\partial t} + \frac{\partial}{\partial x_j} (G_A \rho u_j) = 0$$

【Equation of motion】

$$G_v \frac{\partial}{\partial t} (\rho u_i) + \frac{\partial}{\partial x_j} (G_A \rho u_i u_j) = -G_v \frac{\partial p}{\partial x_i} + \frac{\partial}{\partial x_j} \left[G_A \left(\mu + \mu_T \left(\frac{\partial u_i}{\partial x_j} + \frac{\partial u_j}{\partial x_i} \right) \right) \right] + G_v \rho g_i + C_v \rho F_i + C_v \rho f \varepsilon_{ijk} u_k$$

【Equation of energy transfer】

$$C_p \left[G_v \frac{\partial}{\partial t} (\rho \theta) + \frac{\partial}{\partial x_j} (G_A \rho \theta u_j) \right] = \frac{\partial}{\partial x_j} \left[G_A \left(\lambda + \frac{C_p \mu_T}{Pr_T} \right) \frac{\partial \theta}{\partial x_j} \right] + \frac{1}{P} \left[\sum S_j F_j + Q_s \right]$$

【Equation of vapor transfer】

$$G_v \frac{\partial}{\partial t} (\rho q) + \frac{\partial}{\partial x_j} (G_A \rho q u_j) = \frac{\partial}{\partial x_j} \left[G_A \left(\frac{\mu}{Sc} + \frac{\mu_T}{Sc_T} \right) \frac{\partial q}{\partial x_j} \right] + \left(\sum \frac{S_j F_j}{V} + \frac{Q_i}{\lambda} \right)$$

【Transport equation of turbulent energy】

$$G_v \frac{\partial}{\partial t} (\rho k) + \frac{\partial}{\partial x_j} (G_A \rho k u_j) = \frac{\partial}{\partial x_j} \left[G_A \left(\mu + \frac{\mu_T}{\sigma_k} \right) \frac{\partial k}{\partial x_j} \right] + G_v (P_k + G_k - \rho \varepsilon + \rho F_k)$$

【Transport equation of turbulent energy dissipation rate】

$$G_v \frac{\partial}{\partial t} (\rho \varepsilon) + \frac{\partial}{\partial x_j} (G_A \rho \varepsilon u_j) = \frac{\partial}{\partial x_j} \left[G_A \left(\mu + \frac{\mu_T}{\sigma_\varepsilon} \right) \frac{\partial \varepsilon}{\partial x_j} \right] + G_v \frac{\varepsilon}{k} (C_{\varepsilon 1} P_k + C_{\varepsilon 3} G_k - C_{\varepsilon 2} \rho \varepsilon + C_{\varepsilon 4} \rho F_k)$$

$$\text{Here, } F_i = \alpha C_d g_i \sqrt{u_j^2}, \quad F_k = \alpha C_d \sqrt{\mu_j^3}, \quad \mu_T = \rho C_\mu \frac{k^2}{\varepsilon}$$

$$P_k = \left[\mu_T \left(\frac{\partial u_i}{\partial x_j} + \frac{\partial u_j}{\partial x_i} \right) - \frac{2}{3} \rho k \delta_{ij} \right] \frac{\partial u_i}{\partial x_j}, \quad G_k = \frac{\mu_T}{Pr_T} \frac{g_i}{\theta} \frac{\partial \theta}{\partial x_i} + \frac{\mu_T}{Sc_T} \frac{g_i}{R} \left(\frac{R_0}{M_v} - \frac{R_0}{M_a} \right) \frac{\partial q}{\partial x_i}$$

(Symbols)

- a : Leaf area density [$=1.5[\text{m}^2\text{m}^{-3}]$], C_d : Drag coefficient of tree crown ($=0.2$) [-],
 C_p : Specific heat at constant pressure [$\text{kg}^{-1}\text{K}^{-1}$], F_i : Humidity flux [$\text{kgm}^{-2}\text{s}^{-1}$],
 F_s : Convective sensible heat flux [Wm^{-2}],
 f : Coriolis parameter ($f=2\Omega\sin\phi$, Ω : Angular velocity [rads^{-1}], ϕ : Latitude [rad]) [s^{-1}],
 g : Acceleration due to gravity [ms^{-2}], G_A : Open area ratio on calculation grid interface [-],
 G_v : Volumetric occupancy at the center of calculation grid [-],
 k : Turbulent energy [m^2s^{-2}], λ : Latent heat of vaporization [Jkg^{-1}],
 M_a : Molecular weight of dry air [kgmol^{-1}], M_v : Molecular weight of water [kgmol^{-1}],
 P : Air pressure [Pa], P : Exner function [-], Pr_T : Prandtl number of turbulent flow [-],
 q : Specific humidity [kgkg^{-1}], Q_i : Anthropogenic heat (latent heat) [Wm^{-3}],
 Q_s : Anthropogenic heat (sensible heat) [Wm^{-3}], R : Gas constant [$\text{Jkg}^{-1}\text{K}^{-1}$],
 R_0 : Universal gas constant [$\text{Jmol}^{-1}\text{K}^{-1}$], Sc : Schmidt number ($=0.5$) [-],
 Sc_T : Schmidt number of turbulent flow ($=0.9$) [-], S_q : Area releasing vapor [m^2],
 S_s : Area releasing convective sensible heat [m^2], T : Air temperature [K],
 u_i : i component of wind velocity [ms^{-1}], u_j : j component of wind velocity [ms^{-1}],
 V : Volume of analyzed cell [m^3], ε : Turbulent energy dissipation rate [m^2s^{-3}],
 ε_{ijk} : Eddington's epsilon [-], θ : Potential temperature [K],
 λ : Heat conductivity of air [$\text{Wm}^{-1}\text{K}^{-1}$], μ : Coefficient of viscosity of air [$\text{Pa} \cdot \text{s}$],
 μ_T : Coefficient of eddy viscosity [$\text{Pa} \cdot \text{s}$], ρ : Density [kgm^{-3}]

(Constans)

- $\sigma_k=1.0$, $\sigma_\varepsilon=1.3$, $C_{\varepsilon 1}=1.44$, $C_{\varepsilon 2}=1.3$, $C_{\varepsilon 3}=C_{\varepsilon 1}(G_k \geq 0)$, $C_{\varepsilon 3}=0$ ($G_k < 0$),
 C_{pe1} : Correction coefficient for the resistance coefficient of tree in ε equation ($=1.8$)

Fig. 1 Basic equations.

ground surface was also calculated from the heat balance. An example of judging sunshine is shown in Fig. 2.

2.2 Setting boundary conditions

Boundary conditions could have been set uniformly for the entire upper surface of the analytical space based on dominant wind, but it was decided to assign them for each calculation grid on the upper and side surfaces of the CFD analytical zone and based on the calculation results of a mesoscale model. Each grid on the side boundaries was judged for whether it was inflow or outflow, and calculations were performed for inflow and outflow separately. The u and v pressure components on the upper surface were given based on

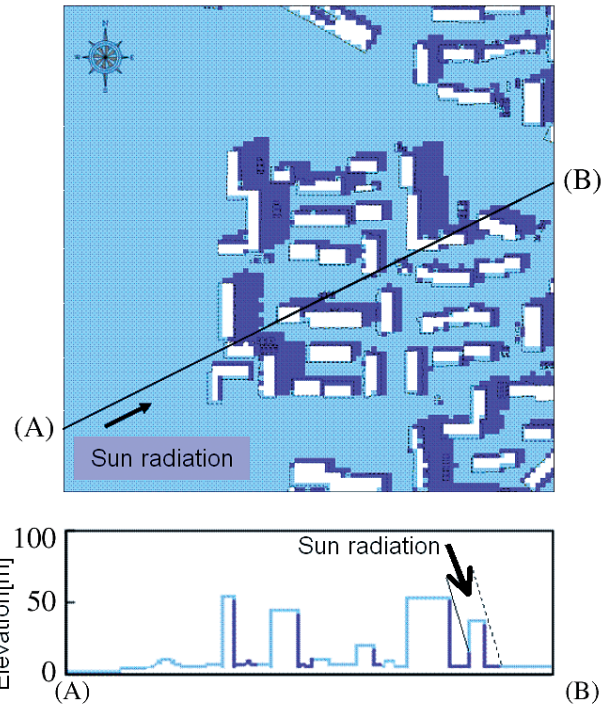


Fig. 2 Example of judging sunshine.

(Whether the ground and building surfaces were in the sun or shade was judged for each grid from the location of the sun, positions of buildings and DEM.)

the results of the mesoscale analysis, but the w component was determined by CFD analysis. The k and ε values on the upper and side surfaces were determined by 1) estimating the wind velocity near the ground surface (0.5 m above the ground surface) using the seventh power law from the wind velocity 500 m above the ground, which was determined by mesoscale analysis, 2) calculating the friction velocity near the ground surface using the logarithmic law, and 3) assuming equilibrium conditions on the upper and side surfaces. In this study, the processes of non-steady phenomena were reflected in the settings of the temperature of the ground surface and boundary conditions, but the fluid field was assumed to be steady within the zone of CFD analysis.

Super high-rise buildings in Tokyo are as tall as 200 m, thus rising above the constant flux layer (the layer near the ground surface where various kinds of flux values are vertically uniform; the layer is usually about 100 m from the ground surface in the daytime). Since the elevation of the ground in Tokyo's 23 wards exceeds 80 m in some districts, a vertical elevation of 300 to 800 m should be analyzed in order to cover all buildings. However, steady calculations can be applied only to limited spaces near the ground surface, and the development of a city boundary surrounded by land and circulating sea air needs to be analyzed for zones above a certain elevation. It is desirable to couple the atmospheric boundary layer and city space, which has a complicated geometrical form, both in non-steady states; however,

such a full-scale calculation method is not possible today and needs to be developed.

3. Classification analysis

The classification analysis was conducted based to the results of Tokyo simulation which covered 33 km square horizontally and from 0 m to 500 m in the vertical direction. The space was divided into grids of 5 m horizontally and 1 to 10 m vertically in the numerical simulation. The total number of grids was about 5 billion (including the buffer zone). It took 16 hours to analyze the zone using 300 calculation nodes.

In order to understand the characteristics of each district from the calculation results, the climatopes were classified by principal component analysis and cluster analysis. Figure 3 illustrates the schema of classification. The classification was performed in the following steps:

- 1) The land use, floor area for each building use, exhaust heat from human activities (latent and sensible heat), air temperature 10 and 100 m above the ground and wind velocity were totalized for each 500-m grid. The mean air temperature and wind velocity of a grid were weighed with effective volume fraction.
- 2) Using the calculated values for each 500-m grid, principal component analysis was performed to quantify the contribution ratio of each principal component.
- 3) Cluster analysis was conducted using the scores of the principal components, and the districts were classified.

The results of classification are shown in Fig. 4. The scores of the first to fifth principal components were used for the cluster analysis. The cumulative contribution ratio was 65%. The characteristics of the six types of district are described below:

Type 1: District of high-rise buildings

Type 2: District where offices, houses and factories coexisted

Type 3: Water district

Type 4: Residential district of detached houses and apartments

Type 5: Industrial district along the coast

Type 6: Forest and river

In Fig. 5, the temperature distribution and aerial photo at Kanda and Nakano were shown. Kanda belongs to type 1, a business district with many high-rise buildings, while Nakano is a typical residential district full of detached houses and apartments. Both of these two districts are located within a distance of less than 10 km from the central Tokyo where many large-scale developments are planned in this area in the near future.

The relationship between air temperature and wind velocity is plotted in Fig. 6 for each type of district. The air temperature difference on the Y axis denotes the mean of the

difference in air temperature between 10 m and 100 m above the ground in the 500-m grid. The mean of the ratio in wind velocity between 10 and 100 m above the ground in the 500-m grid is shown on the X axis. The temperature difference was smaller at a larger wind velocity ratio. At a wind velocity ratio of about 1, the temperature difference converged to 1°C and was similar to the temperature drop with elevation. This trend was observed in Type 3 districts. On the other hand, in districts of small wind velocity ratio, the vertical temperature difference was as large 4 to 5°C. This trend was observed in many Type 1 districts, showing that closely spaced buildings affected the ventilation and air temperature in the districts.

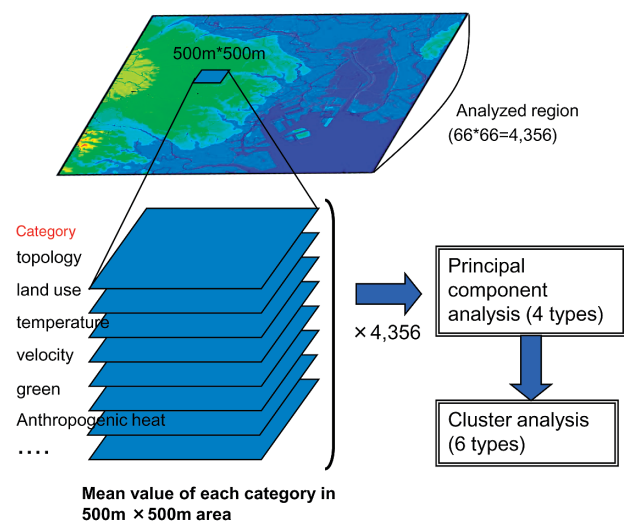


Fig. 3 Classification of Climatope by principal component analysis and cluster analysis.

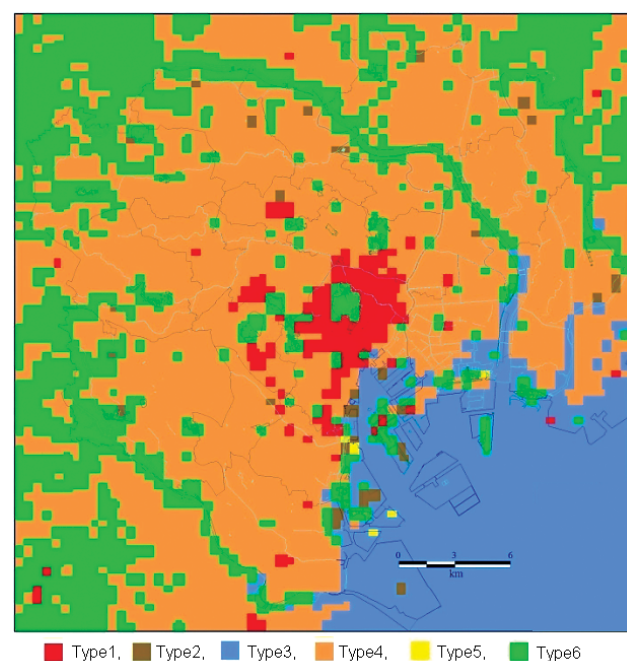


Fig. 4 Classification result.



Fig. 5 Temperature distribution and aerial photo at Kanda and Nakano.

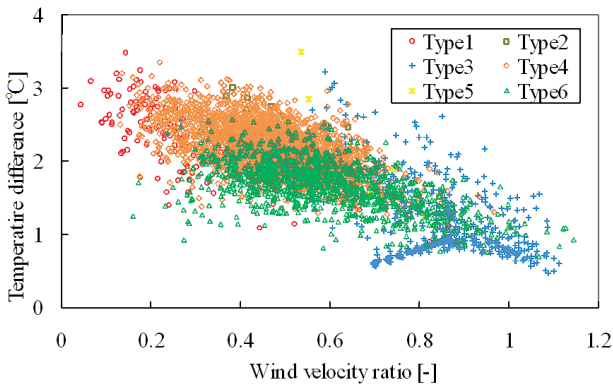


Fig. 6 Relationship between wind velocity and air temperature (500-m grid)
(y-axis is the difference of air temperature at 10 m and 100 m over ground; x-axis indicates the ratio of wind velocity at 10 m and 100 m over ground)

4. Conclusions

A numerical simulation consisting of about 5 billion grids was performed using the Earth Simulator to clarify the distribution of air temperature and wind velocity in Tokyo's 23 wards. A close relationship was found between air tempera-

ture and wind velocity. Using the result of numerical simulation, cluster analysis and principle component analysis were employed to classify climatopes, for each of which the relationship between air temperature and wind velocity was analyzed. The cumulative contribution ratio of the first fifth principal components was 65%. The result of cluster analysis and principal component analysis pointed out that land uses play a key role in formation of local climate.

Now, a night-time simulation is under running on the Earth Simulator. The further analysis including the conditions at night is expected in the near future.

References

- [1] Yasunobu ASHIE, Nobuyoshi KOMATSU, Takaaki KONO and Keiko TAKAHASHI: Numerical simulation of urban thermal environment in the waterfront area of Tokyo, Annual report of the earth simulator center April 2005 - March 2006, The Earth Simulator Center (JAM-STE), pp.83-87, 2007.1, ISSN 1348-5822.
- [2] Yasunobu ASHIE, Takayuki TOKAIRIN, Takaaki KONO and Keiko TAKAHASHI: Numerical simulation of urban heat island in a ten-kilometer square area of

central Tokyo, Annual report of the earth simulator center April 2006 - March 2007, The Earth Simulator Center (JAMSTEC), pp.45-48, 2007.10, ISSN 1348-5822.

[3] Kohin HIRANO, Takaaki KONO and Yasunobu ASHIE:

Large-scale CFD Simulation of Heat Island Phenomenon and Countermeasures in Tokyo, Annual report of the earth simulator center April 2007 - March 2008, The Earth Simulator Center (JAMSTEC), 2008.

東京23区の大規模CFD計算及びクリマトープの類型化処理

プロジェクト責任者

足永 靖信 建築研究所 環境研究グループ

著者

平野 洪賓*¹, 河野 孝昭*¹, 足永 靖信*¹

*¹ 建築研究所 環境研究グループ

筆者らは、都市のヒートアイランド現象を詳細に解析するため、土地被覆、建物高さ、人工排熱等の都市要素の影響を分析可能な数値解析システムを地球シミュレータ上に構築し、これまでに5km四方、10km四方、33km四方の解析領域を設定して数値シミュレーションを実施してきた。今年度は東京23区全域をカバーする33km四方領域の数値シミュレーション結果に対して街区スケールの熱環境特性を明らかにするためのクラスター分析を実施した。分析は500m四方の街区における都市情報(緑被率、建ぺい率、建物高さ、標高等)及び環境要素(風速、気温等)に基づく。上位5成分による累積寄与率は65%であり、土地利用形態がローカルスケールの気候の形成に最も大きな影響を与えていることが判明した。

キーワード: ヒートアイランド, CFD, 類型化, クラスター分析, 主成分分析